Electronic structure of the misfit-layer compound $(SnS)_{1.17}NbS_2$ deduced from band-structure calculations and photoelectron spectra

C. M. Fang, A. R. H. F. Ettema, C. Haas, and G. A. Wiegers
Laboratory of Chemical Physics, Materials Science Center, University of Groningen, Nijenborgh 4, 9747 AG Groningen, The Netherlands

H. van Leuken and R. A. de Groot
ESM, Research Institute for Materials, Toernooiveld 9, 6525 ED Nijmegen, The Netherlands
(Received 11 October 1994)

In order to understand the electronic structure of the misfit-layer compound $(SnS)_{1.17}NbS_2$ we carried out an *ab initio* band-structure calculation of the closely related commensurate compound $(SnS)_{1.20}NbS_2$. The band structure is compared with calculations for NbS_2 and for hypothetical SnS with structure and interatomic distances as in $(SnS)_{1.20}NbS_2$. The calculations show that the electronic structure is approximately a superposition of the electronic structures of the two components NbS_2 and SnS, with a small charge transfer from the SnS layer to the NbS_2 layer. The interlayer bonding between SnS and NbS_2 is dominated by covalent interactions. X-ray and ultraviolet photoelectron spectra were obtained for the valence bands. The observed spectra are in good agreement with the band-structure calculations.

I. INTRODUCTION

The misfit-layer compounds form a class of compounds with general formula $(MX)_{1+x}TX_2$ (M=Sn, Pb, Bi, Sb, or rare-earth metal; X=S, Se; T=Ti, V, Cr, Nb, Ta; and $0.08<x<0.23$) and planar intergrowth structures. These compounds lack three-dimensional periodicity.[1-3] Previously it was thought that these compounds have the stoichiometry MTX_3, but extensive x-ray diffraction studies showed that they are built of alternating double layers MX and sandwiches TX_2, which do not match. A remarkable feature is that they are very stable. For a better understanding of the stability of the misfit-layer compounds and the chemical bonding between the two subsystems MX and TX_2 an electronic band structure is important.

Wiegers *et al.* showed that $(SnS)_{1.17}NbS_2$ is built of two-atom-thick layers of SnS and three-atom-thick sandwiches of NbS_2; both have C-centered orthorhombic unit cells which do not match along the in-plane [100] direction.[4-6] $(SnS)_{1.17}NbS_2$ has p-type metallic electronic conduction, with a hole concentration of about 0.87 holes/Nb deduced from Hall effect measurements, similar to 2H-NbS_2.[4] On the basis of x-ray photoemission (XPS), x-ray absorption, and electron-energy-loss studies, Ohno concluded the presence of charge transfer from the SnS to the NbS_2 layer and found that the valence-band structure is well represented by a simple superposition of the electronic structure of each layer, except for charge-transfer effects.[7] From XPS Ettema and Haas concluded that interlayer charge transfer is absent or small, and that the stability is due to covalent interlayer bonds.[8] From Raman scattering of the misfit compounds $(SnS)_{1.17}NbS_2$, $(PbS)_{1.14}NbS_2$, and $(PbS)_{1.18}TiS_2$ Hangyo and co-workers found that the spectra obtained can be regarded as a superposition of the intralayer vibrations of individual layers, which indicates a weak interlayer interaction. The shift of the interlayer Raman modes of NbS_2 in the misfit compounds relative to those of 2H-NbS_2 was interpreted in terms of a charge transfer from the MS layer to the TS_2 layer.[9,10]

So far there are no reports on band-structure calculations for misfit compounds. In this work we present a study of the electronic structure of the misfit compound $(SnS)_{1.17}NbS_2$ using *ab initio* band-structure calculations and photoelectron spectra.

II. STRUCTURE OF $(SnS)_{1.17}NbS_2$

The two subsystems, SnS and NbS_2, of $(SnS)_{1.17}NbS_2$ are characterized by C-centered orthorhombic unit cells given in Table I.[1,2] The in-plane axes are **a** and **b**. The corresponding axes of the two subsystems are parallel and equal for **b** and **c**, but the **a** axes have an incommensurate length ratio. Coordinates of the atoms are given in Table II. The SnS part of the structure consists of deformed slices of SnS with a thickness of half the cell edge of (hypothetical) distorted NaCl-type SnS. Each Sn atom is coordinated by five S atoms, four S atoms are in a plane perpendicular to the **c** axis with Sn-S distances 2.774(1)(1×), 2.874(1)(2×), and 3.047(1)(1×) Å, whereas the fifth Sn-S bond with length 2.696(9) Å is approximately along the **c** axis. The NbS_2 part of the structure is that of 2H-NbS_2, with Nb in a trigonal-prismatic

TABLE I. Unit-cell dimensions, space group (S.G.), and number Z of formula units of the subsystems of $(SnS)_{1.17}NbS_2$.

	a (Å)	b (Å)	c (Å)	S.G.	Z
SnS	5.673	5.751	11.761	$Cm2a$	4
NbS_2	3.321	5.751	11.761	$Cm2m$	2

0163-1829/95/52(4)/2336(12)/$06.00

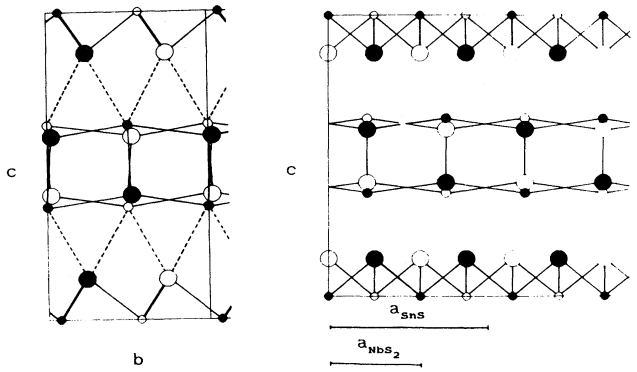

FIG. 1. Crystal structure of $(SnS)_{1.17}NbS_2$. Small circles are Nb (at the bottom and top) and Sn (in the middle), large circles are S atoms. Atoms of the same subsystem $a/2$ apart are indicated by open and filled circles of the same size. Dashed lines indicate the interaction of Sn with S of NbS_2 layer. (a) (left): projection along [100]. The SnS double layer is situated at $z=\frac{1}{2}$. (b) (right): projection along [010] showing the incommensurate character along [100]. The SnS double layer is situated at $z=\frac{1}{2}$.

coordination of S; the Nb-S distances are 2.473(1) Å. The composition of the misfit compound is determined by the ratio of the **a** axes of the two subsystems, viz., $1.17=(3.321/5.673)\times(4/2)$, 4/2 being the ratio of the number of formula units per cell of the two subsystems. Projections of the structure along [100] and [010] are shown in Figs. 1(a) and 1(b). The two subsystems mutually modulate each other incommensurately, which means that the structure obtained from the three-dimensional space groups of the two subsystems gives only the average structure of the misfit-layer compound. The complete structure, including the mutual modulation, is described by a (3+1)-dimensional superspace group.[3,6] Compared to the average structure, the distances are slightly modulated as was demonstrated for $(PbS)_{1.18}TiS_2$.[11] In the case of $(SnS)_{1.17}NbS_2$ the modulation parameters were not determined and the average structure had to be used for a band-structure calculation.

TABLE II. Fractional coordinates of $(SnS)_{1.17}NbS_2$ for the atoms in the subsystems SnS and NbS_2, expressed in terms of the unit cells of the subsystems of Table I. W.P. is the Wyckoff position.

	W.P.	x	y	z
		SnS		
Sn	4(c)	$\frac{1}{4}$	0	0.6335
S(1)	4(c)	$\frac{1}{4}$	0.476	0.5954
		NbS_2		
Nb	2(a)	0	−0.075	0
S(2)	4(c)	0	0.2585	0.1328

Since the existing computer programs for band-structure calculations cannot be used to calculate the electronic structure of modulated crystals, or other solids without three-dimensional translation periodicity, the most simple way to perform a calculation of the band structure is to make the incommensurate crystal structure commensurate. This can be achieved by approximating the structure with a large unit cell. For $(SnS)_{1.17}NbS_2$ the simplest commensurate approximation consists of 5 units NbS_2 and 3 units SnS along [100], $a=16.605$ Å ($=5a_{NbS_2}\approx 3a_{SnS}$), $b=5.751$ Å, $c=11.761$ Å, and, as a consequence, a composition $(SnS)_{1.20}NbS_2$. The c axis was perpendicular to the **ab** plane. The a axis was chosen equal to five times that of a_{NbS_2} since the NbS_2 part in misfit-layer compounds is the more rigid one of the two subsystems. The SnS part is thus slightly compressed (2.5%). In the commensurate supercell, the origin along [100] of one lattice with respect to the other can be chosen arbitrarily; an arbitrary choice leads to a C-centered lattice with 6 Sn, 5 Nb, and 16 S as crystallo-

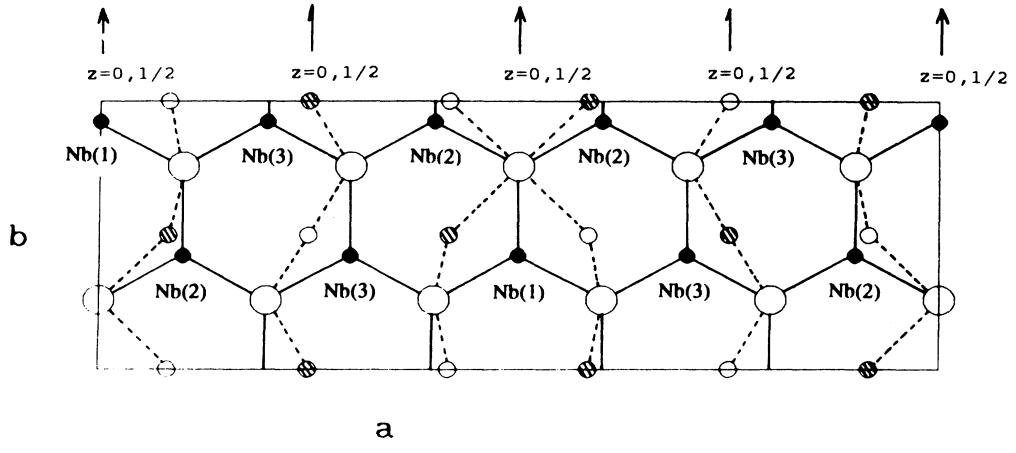

FIG. 2. Projection of $(SnS)_{1.20}NbS_2$ along [001] in the large supercell, space group $C2$. Large open circles are S atoms of the NbS_2 subsystem. Sulfur atoms of the SnS subsystem are not indicated for the sake of clarity. Small open (hatched) and filled circles are Sn and Nb, respectively. Sn atoms at z and $-z$ are indicated by open and hatched circles.

graphically independent atoms [cell content $(SnS)_{12}(NbS_2)_{10}$]. By choosing the origin of SnS with respect to NbS_2 as shown in Fig. 2, the arrangement is described in the monoclinic space group $C2$. All atoms are on general sites $4(c)$, except Nb(1), which is on site $2(a)$. The number of crystallographically independent atoms is therefore reduced to 3 Nb, 3 Sn, and 8 S atoms.

III. BOND LENGTH AND BOND STRENGTH

The bond distances of the misfit compound $(SnS)_{1.17}NbS_2$ are listed in Table III. The bond distances in the large unit cell of $(SnS)_{1.20}NbS_2$ used for band-structure calculations are included for comparison. Some insight into the bonding can be obtained by using the concept of bond valence.[12] The bond valence V_i is calculated from the relation $V_i=\exp[(d_0-d_i)/b]$, where d_i is the distance between the atoms of bond i, and d_0 and b are empirical constants: $d_0=2.45$ Å for Sn-S, $d_0=2.37$ Å for Nb-S, and $b=0.37$.[13] The bond valence or oxidation state V of an atom is calculated by summing over all neighboring atoms $V=\sum V_i$.

The calculated bond valences of Sn and S are given in Table III. The interatomic distances and bond valences for $x=0.20$ (commensurate, large unit cell) and $x=0.17$ (incommensurate misfit compound) are the same, except for two Sn-S bonds parallel to [100], which are shorter due to the compression along [100].

The Sn-S bond distances and corresponding bond valences are quite different in α-SnS, β-SnS, and the intergrowth compounds $(SnS)_{1+x}$ NbS_2 ($x=0.17$ and 0.20). The sum $\sum V_i$ of the contributions of intralayer Sn-S bonds to the valence of Sn is somewhat smaller for $(SnS)_{1+x}NbS_2$ (1.89 for $x=0.20$; 1.77 for $x=0.17$) than for α-SnS (1.94) and β-SnS (1.81).

In α- and β-SnS there is very weak interlayer bonding, with $V=0.079$ for α-SnS (one interlayer Sn-S bond of 3.388 Å) and $V=0.072$ for β-SnS (two interlayer Sn-S bonds of 3.74 Å). The interlayer bonding in the misfit-layer compounds is much stronger. For $(SnS)_{1.20}NbS_2$ the contribution of interlayer bonds to the Sn valence is 0.245, 0.238, and 0.256 for Sn(1), Sn(2), and Sn(3), respectively. In the incommensurate structure ($x=0.17$) the interlayer Sn-S bond valence shows a continuous range of values; the average value is about 0.24, close to the average value for $x=0.20$.

The total valence of Sn in $(SnS)_{1+x}NbS_2$, obtained by adding the contributions of interlayer and intralayer bonds, is about two, close to the values in α- and β-SnS.

IV. BAND-STRUCTURE CALCULATIONS

A. Method of the calculations

Ab initio band-structure calculations were performed with the localized spherical wave (LSW) method[15] using a scalar-relativistic Hamiltonian. The LSW method is a modified version of the augmented spherical wave method.[16] We used local-density exchange-correlation potentials[17] inside space filling, and therefore overlapping spheres around the atomic constituents. The self-consistent calculations were carried out including all core electrons.

Iterations were performed with **k** points distributed

TABLE III. Interatomic distances d_i (Å) and bond valences V_i in the misfit-layer compound $(SnS)_{1+x}NbS_2$ for $x=0.17$ and 0.20, compared with α- and β-SnS.

1. Bonds in layers

$x=0.20$ (comm.)		$x=0.17$ (incomm.)	
d_i (Å)	V_i	d_i (Å)	V_i
2×2.806	0.382	2×2.874	0.376
1×2.774	0.417	1×2.774	0.417
1×3.047	0.199	1×3.047	0.199
1×2.696	0.514	1×2.696	0.514
$V=\sum V_i$	1.89		1.77

2. Bonds between Sn in the SnS layer and S in the NbS_2 layer ($x=0.20$)

Sn(1)		Sn(2)		Sn(3)	
d_i	V_i	d_i	V_i	d_i	V_i
1×3.417	0.073	1×3.376	0.082	1×3.233	0.120
1×3.108	0.169	1×3.137	0.156	1×3.189	0.136
$V=\sum V_i$	0.245		0.238		0.256

3. Sn-S bonds in α- and β-SnS

α-SnS		β-SnS	
d_i (Å)	V_i	d_i (Å)	V_i
1×2.627	0.620	1×2.59	0.685
2×2.665	0.559	4×2.96	0.281
2×3.290	0.103	2×3.74	0.036
1×3.388	0.079		
$V=\sum V_i$	2.02		1.88

TABLE IV. Input parameters for the band-structure calculation of $(SnS)_{1.20}NbS_2$. W.P. is the Wyckoff position. The empty spheres are indicated by Va, the radii of the muffin-tin spheres of Sn, Nb, and S by R_{WS} (Å). Super cell space group $C2$ (No. 5). $a=16.605$ Å. $b=5.751$ Å; $c=11.761$ Å; $V=1123.12$ Å^3; cell content $(SnS)_{12}(NbS_2)_{10}$.

Atoms	W.P.	Coordinates	R_{WS} (Å)
Nb(1)	2*a*	(0.0,0.925,0.0)	1.223
Nb(2)	4*c*	(0.1,0.425,0.0)	1.223
Nb(3)	4*c*	(0.2,0.925,0.0)	1.223
S(1)	4*c*	(0.0,0.2585,0.1328)	1.772
S(2)	4*c*	(0.1,0.7585,0.1328)	1.772
S(3)	4*c*	(0.1,0.7585,0.8672)	1.772
S(4)	4*c*	(0.2,0.2585,0.1328)	1.772
S(5)	4*c*	(0.2,0.2585,0.8328)	1.772
Sn(1)	4*c*	(0.0833,0.0,0.6335)	1.275
Sn(2)	4*c*	(0.0833,0.5,0.3665)	1.275
Sn(3)	4*c*	(0.2500,0.0,0.3665)	1.275
S(6)	4*c*	(0.0833,0.4760,0.5954)	1.931
S(7)	4*c*	(0.0833,0.9760,0.4046)	1.931
S(8)	4*c*	(0.2500,0.4760,0.4046)	1.931
Va(1)	2*b*	(0.0,0.2240,0.5)	0.80
Va(2)	2*b*	(0.0,0.7240,0.5)	0.80
Va(3)	4*c*	(0.16667,0.2260,0.5)	0.80
Va(4)	4*c*	(0.16667,0.7260,0.5)	0.80
Va(5)	2*a*	(0.0,0.5927,0.0)	1.08
Va(6)	4*c*	(0.1,0.0877,0.0)	1.08
Va(7)	4*c*	(0.2,0.5827,0.0)	1.08
Va(8)	4*c*	(0.1335,0.1640,0.7229)	0.80
Va(9)	4*c*	(0.8430,0.6230,0.7230)	0.80

uniformly in an irreducible part of the first Brillouin zone (BZ), corresponding to a volume of the BZ per **k** point of the order of 5×10^{-5} Å^{-3}. Self-consistency was assumed when the changes in the local partial charges in each atomic sphere decreased to the order of 10^{-4}.

In the construction of the LSW basis,[15,18] the spherical waves were augmented by solutions of the scalar-relativistic radial equations indicated by the atomiclike symbols 5*s*, 5*p*, 5*d*; 5*s*, 5*p*, 4*d*; and 3*s*, 3*p*, 3*d* corresponding to the valence levels of the parent elements Sn, Nb, and S, respectively. The internal l summation used to augment a Hankel function at surrounding atoms, was extended to $l=3$, resulting in the use of 4*f* orbitals for Sn and Nb. When the crystal is not very densely packed, as is the case in the layered materials like $(SnS)_{1.17}NbS_2$, NbS_2, and SnS, it is necessary to include empty spheres in the calculations. The functions 1*s*, 2*p*, and 3*d* as an extension were used for the empty spheres. The input parameters (lattice constants, Wigner-Seitz sphere radii) are listed in Table IV.

B. The band structures of the two components NbS_2 and SnS

For a better understanding of the band structure of $(SnS)_{1+x}NbS_2$ it is useful to compare the results of the calculations with band structures of the two components SnS and NbS_2. Detailed calculations were reported for α- and β-SnS.[14] However the structure of the SnS double layers in α- and β-SnS is quite different from that in the misfit-layer compound $(SnS)_{1+x}NbS_2$. Therefore we have carried out band-structure calculations for hypothetical SnS crystal structures, similar to the structure incorporated in the misfit-layer compounds.

In the band-structure calculation of the misfit-layer compound $(SnS)_{1+x}NbS_2$ we have approximated the incommensurate structure ($x=0.17$) by a commensurate structure with a large unit cell ($x=0.20$). We remark that with this approximation we neglect the complicated effects (such as the localization of electrons) which are essentially due to the incommensurability of the crystal structure.[19] These effects are expected to be small for the chemical bonding to be discussed in this paper, but they may play an important role in the electronic transport properties. In the large unit cell ($x=0.20$) the NbS_2 part is kept the same as that in the incommensurate structure. However, the SnS part was changed a little, two of the Sn-S bonds were shortened by about 0.068 Å. To understand the effect of this small compression we calculated the band structures of two hypothetical SnS structures, one with the structure as in the misfit-layer compound

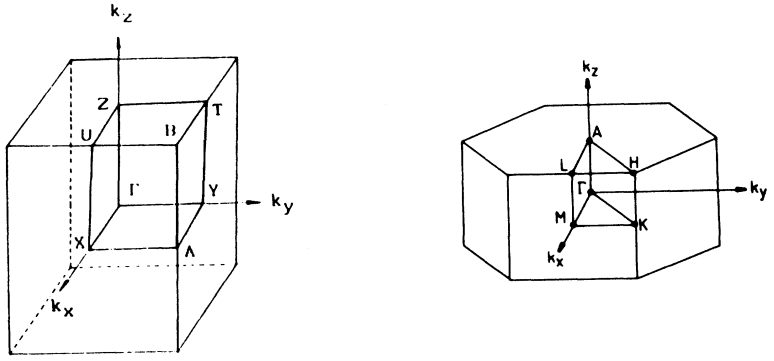

(a) (b)

FIG. 3. Brillouin zones and high symmetry points of (a) SnS-1 and SnS-2, and (b) 2H-NbS_2.

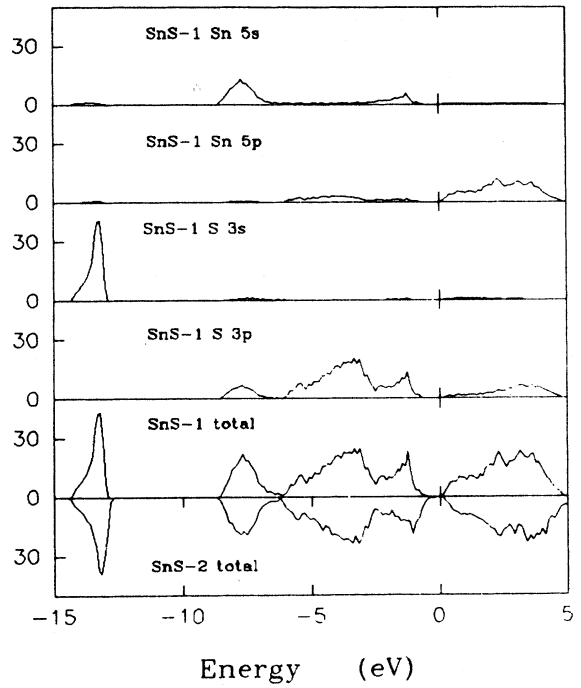

FIG. 4. The total and partial densities of states of SnS-1 ($a=5.673$ Å), and the total density of states of SnS-2 ($a=5.535$ Å).

with $x=0.17$ (SnS-1; $a=5.673$ Å), and one with the structure as in the commensurate compound with $x=0.20$ (SnS-2, $a=5.535$ Å). The Brillouin zone of SnS-1 and SnS-2 is given in Fig. 3(a). These hypothetical SnS structures have the same space group $Cm2a$ as the SnS subsystem in $(SnS)_{1+x}NbS_2$. The input parameters for band-structure calculations of SnS-1 and SnS-2 are given in Table V.

TABLE V. Input parameters for band-structure calculations of hypothetical SnS.

SnS-1					SnS-2
		Space group			
$Cm2a$					$Cm2a$
$a=5.673$ Å					$a=5.535$ Å
$b=5.751$ Å					$b=5.751$ Å
$c=6.281$ Å					$c=6.281$ Å
		Coordinates		SnS-1	SnS-2
	x	y	z	R_{WS} (Å)	R_{WS} (Å)
Sn 4c	($\frac{1}{4}$,	0,	0.2500)	1.488	1.488
S 4c	($\frac{1}{4}$,	0.476,	0.1786)	1.671	1.671
$V1$ 4a	(0,	0.250,	0.0000)	0.940	0.940
$V2$ 4a	(0,	0.250,	0.5000)	1.510	1.311

The density of states (DOS) of the two hypothetical structures are compared in Fig. 4. The dispersion of the energy bands of SnS-1 is shown in Fig. 5. SnS-1 is a semiconductor like α- and β-SnS.[14] The sulfur 3s states are clearly separated from the other states of the valence band by a gap of 4.2 eV, which is larger than the value for β-SnS (3.5 eV) or α-SnS (4.0 eV). The valence band is composed of strongly hybridized S 3p, Sn 5s, and Sn 5p orbitals. The bottom and top of the valence band consist of Sn 5s and S 3p, which is characteristic for the existence of Sn 5s lone pairs. The bands in the middle of the valence band consist mainly of S 3p and Sn 5p states. The energy gap is about 0.6 eV, which is smaller than the calculated energy gap of α-SnS (1.6 eV) but larger than that of β-SnS (0.3 eV). The band structure of SnS-2 is compared with that of SnS-1 in Fig. 4. The band structure of SnS-2 is almost the same as that of SnS-1, but the width of the valence band of SnS-2 is about 0.20 eV larger than that of SnS-1.

For 2H-NbS_2 a linear muffin-tin-orbital calculation of

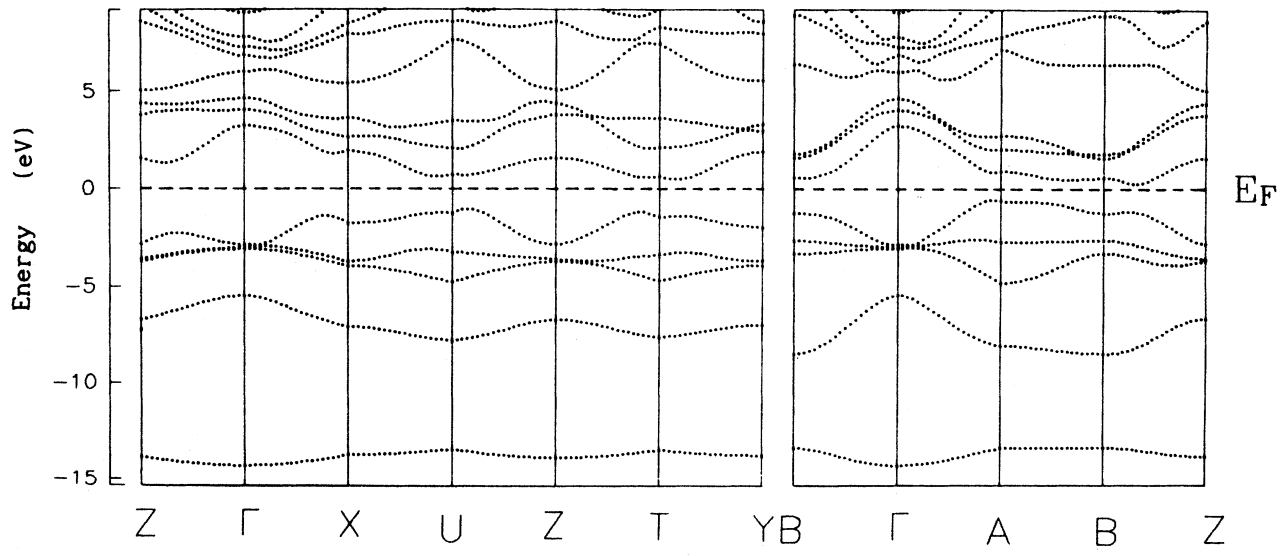

FIG. 5. Dispersion of the energy bands of SnS-1.

TABLE VI. Input parameters for the band-structure calculation of 2H-NbS_2.

	Coordinates			R_{WS} (Å)
	x	y	z	
Nb 2*b*	0	0	$\frac{1}{4}$	1.30
S 4*f*	$\frac{1}{3}$	$\frac{2}{3}$	0.1180	1.60
*V*1 2*d*	$\frac{1}{3}$	$\frac{2}{3}$	$\frac{3}{4}$	0.92
*V*2 2*a*	0	0	0	0.92

the band structure by Kasowski is available.[20] In order to make a comparison with the band structure of the misfit-layer compound we have calculated the band structure of 2H-NbS_2 using the LSW method. The space group of 2H-NbS_2 is $P6_3/mmc$, the unit cell parameters $a=b=3.324$ Å, $c=11.95$ Å.[21] The input parameters of the calculations are given in Table VI, the Brillouin zone is given in Fig. 3(b). The dispersion of the energy bands of 2H-NbS_2 is shown in Fig. 6, the density of states in Fig. 7. The obtained band structure of 2H-NbS_2 is quite different from that reported by Kasowski,[20] but it is very similar to the band structure of 2H-TaS_2 obtained by the augmented plane-wave method.[22] For an extensive discussion of the transition-metal *d* bands in layered transition-metal dichalcogenides, we refer to Refs. 22 and 23. In the band structure of 2H-NbS_2 the S 3*s* states dominate the four bands with lowest energy. These bands are separated by a gap of 5.3 eV from the highest valence bands which consist mainly of S 3*p* orbitals. The lowest Nb 4*d* states form the so-called Nb $4d_{z^2}$ bands. The Nd $4d_{z^2}$ band has a large contribution of Nb $4d_{z^2}$ states, but it contains also contributions from other Nb 4*d* states. The Nb $4d_{z^2}$ band is half-filled, so that there is one hole per Nb atom.

C. Band structure of $(SnS)_{1.17}NbS_2$

The first Brillouin zone of the structure in the large unit cell with space group *C*2 (No. 5) is shown in Fig. 8; the **c*** axis in reciprocal space is perpendicular to the **a*b*** plane, as in the real structure of $(SnS)_{1.17}NbS_2$. The dispersion of the energy bands near the Fermi level and of the sulfur 3*s* state band is shown in Fig. 9 for selected directions in the BZ. The energy bands nicely reflect the symmetry of the twofold axis; the dispersion is the same for Γ-*X* and Γ-*Y*, for *U*-*X* and *T*-*Y*, and for *U*-*Z* and *T*-*Z*. The total and partial density of states obtained from the band-structure calculations is shown in Fig. 10. The charges in the Wigner-Seitz spheres and the orbital configuration of atoms and empty spheres are given in Table VII. We remark that not too much significance should be attributed to differences in charge and orbital configuration, as these numbers are strongly dependent on the Wigner-Seitz radii, and the presence of empty spheres. The variation of the electronic configuration of one type of atom within a subsystem is small; this indicates that the modulation of the electronic structure of one subsystem by the other subsystem is small. There is a

TABLE VII. Electronic configurations of the atoms in $(SnS)_{1.20}NbS_2$.

Atom	R_{WS} (Å)	Electronic configuration
NbS_2-subsystem		
Nb(1)	1.223	$[Kr]5s^{0.12}5p^{0.18}4d^{1.99}4f^{0.03}$
Nb(2)	1.223	$[Kr]5s^{0.12}5p^{0.18}4d^{2.00}4f^{0.03}$
Nb(3)	1.223	$[Kr]5s^{0.12}5p^{0.18}4d^{2.00}4f^{0.03}$
S(1)	1.772	$[Ne]3s^{1.93}3p^{4.92}3d^{0.30}4f^{0.00}$
S(2)	1.772	$[Ne]3s^{1.93}3p^{4.91}3d^{0.31}4f^{0.00}$
S(3)	1.772	$[Ne]3s^{1.93}3p^{4.92}3d^{0.31}4f^{0.00}$
S(4)	1.772	$[Ne]3s^{1.93}3p^{4.93}3d^{0.31}4f^{0.00}$
S(5)	1.772	$[Ne]3s^{1.93}3p^{4.90}3d^{0.31}4f^{0.00}$
SnS-subsystem		
Sn(1)	1.275	$[[Kr]4d^{10}]5s^{1.17}5p^{0.40}5d^{0.07}4f^{0.01}$
Sn(2)	1.275	$[[Kr]4d^{10}]5s^{1.18}5p^{0.41}5d^{0.07}4f^{0.01}$
Sn(3)	1.275	$[[Kr]4d^{10}]5s^{1.21}5p^{0.39}5d^{0.07}4f^{0.01}$
S(6)	1.931	$[[Ne]3s^{2.03}3p^{5.12}3d^{0.60}4f^{0.00}$
S(7)	1.931	$[Ne]3s^{2.01}3p^{5.17}3d^{0.52}4f^{0.00}$
S(8)	1.931	$[Ne]3s^{2.03}3p^{5.15}3d^{0.47}4f^{0.00}$

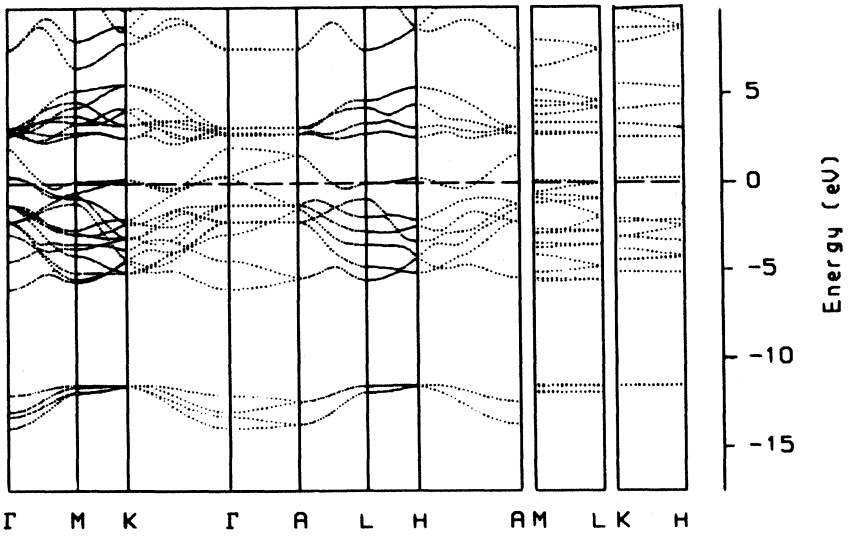

FIG. 6. Dispersion of the energy bands of 2H-NbS_2.

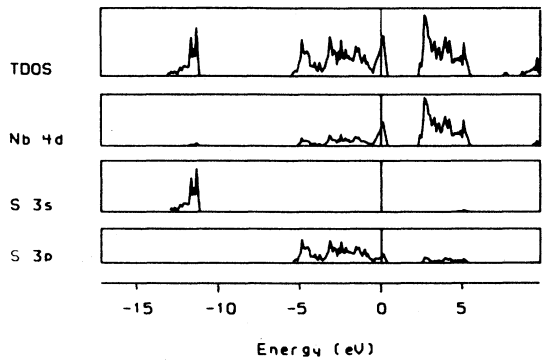

FIG. 7. Total and partial densities of states of 2H-NbS_2.

small but significant difference between the electronic configurations of S in the NbS_2 and SnS subsystems, but this is at least partly due to the different Wigner-Seitz radii.

In the total density of states we can distinguish two separate sets of energy bands. The lowest bands mainly consists of sulfur 3*s* orbitals, with in the lower part mainly S 3*s* of the NbS_2 subsystem, whereas the S 3*s* states of the SnS subsystem are at the top of these bands. There is a shift of about 0.8 eV to lower energy of the top of the S 3*s* band of the NbS_2 subsystem in the misfit-layer compound with respect to the bottom of the Nb $4d_{z^2}$ band, as compared with 2H-NbS_2. This shift could be due to a lowering of the S 3*s* orbital energy by Coulomb interaction with Sn.

The energy gap between the S 3*s* band and the valence band is about 4.2 eV, which is smaller than for 2H-NbS_2 (about 5.3 eV), but it is the same as for the band structures of the hypothetical SnS in Figs. 4 and 5. The valence band ranges from −7.70 to +0.85 eV, with a width of about 8.55 eV, which is much larger than that of 2H-NbS_2 (where it is about 6.0 eV). The partial band structure of the SnS part is very similar to that of the SnS-2. The bottom of the partial DOS of the SnS part consists for a large part of Sn 5*s* and S 3*p* states. The middle part of the valence band consists mainly of S 3*p* states, hybridized with Sn 5*p* states. The top of the band of the SnS part consists of S 3*p* hybridized with Sn 5*s*. These results indicate that the partial band structure of SnS in the misfit structure is similar to that of the hypothetical SnS structure, with a shift to higher energy of about 0.9 eV. The valence band of the NbS_2 subsystem consists of S 3*p* and Nb 4*d*, similar to that of the 2H-NbS_2. However, the gap between the S 3*s* bands and the valence band is smaller than in 2H-NbS_2 and the valence band starts at an energy 2.5 eV lower than in 2H-NbS_2. The lower part of the valence band consists mainly of Sn 5*s* and S 3*p* of the SnS subsystem, and a small contribution of S 3*p* of the NbS_2 subsystem. The latter contribution is direct evidence for a covalent interlayer interaction between Sn 5*s* and S(NbS_2) 3*p* orbitals.

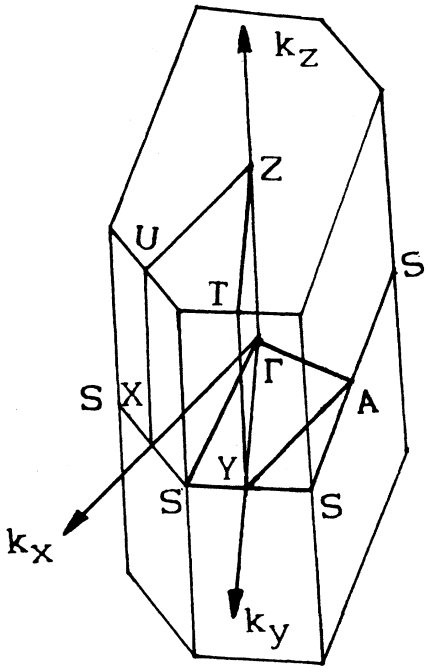

FIG. 8. Brillouin zone and high symmetry points of $(SnS)_{1.20}NbS_2$ with space group *C*2.

The energy bands near the Fermi level are mainly composed of Nb 4*d*, S 3*p* orbitals of the SnS and NbS_2 subsystems, and Sn 5*s* states. The hypothetical SnS-2 compound is a semiconductor. However, in the calculated band structure of $(SnS)_{1.20}NbS_2$ there are unoccupied 3*p* states of sulfur atoms in the SnS subsystem, and also unoccupied Sn 5*s* states, which indicate charge transfer from SnS to NbS_2. If we take the unoccupied Sn 5*s* states as the charge transferred from the SnS layer to the NbS_2 layer, the transferred charge amounts to about 0.15 electron per Nb. If we count the sum of the unoccupied states of Sn 5*s* and S 3*p* orbitals of the SnS subsystem as layer-to-layer charge transfer, the charge transferred would amount to 0.5 electron/Nb. The amount of charge transfer may be a little smaller if the compression effect is taken into account.

Figure 9 shows the dispersion curves of the electronic structure of the misfit-layer compound $(SnS)_{1.20}NbS_2$ in selected directions. The S 3*s* bands show very little dispersion along the Γ-*Z*, *T*-*Y*, and *X*-*U* directions parallel to the **c*** axis. This is understandable because in the directions parallel to *c**, the S-S distances are too long for strong interlayer 3*s*-3*s* interactions. The six top bands mainly consist of S 3*s* of the SnS part and the lower ten bands are mainly of S 3*s* of the NbS_2 subsystem. In the intermediate region there exists a hybridization between S 3*s* orbitals of the SnS and NbS_2 subsystems for directions perpendicular to **c***. However, this hybridization does not contribute to net interlayer bonding, because all bonding and antibonding states are occupied.

The bands near the Fermi level show a strong dispersion for directions with a **k** component perpendicular to **c***. This dispersion is caused by strong covalent intralayer interactions in the subsystems, and is also found in the band structures of the components. Near the top

of the valence band we observe several bands with a dispersion, of about 0.5–1.0 eV. These are presumably the bands with mainly Nb 4*d* character. Some of the bands show a large dispersion, with a change of energy of 1–2 eV over the narrow range Γ-*X* in the Brillouin zone of the misfit-layer compound. These are probably bands derived from the top of the valence band of the SnS subsystem. The dispersion curves also show uncrossing of these bands at intersections, which corresponds to covalent interlayer interactions.

The bands at the Γ point of the Brillouin zone with (mainly) Nb $4d_{z^2}$ character are at energies of −0.09, −0.09, −0.46, −0.48, and −1.60 eV. These bands correspond to the Nb $4d_{z^2}$ states of the five Nb atoms in the primitive unit cell of $(SnS)_{1.20}NbS_2$. The spread of the energies over 1.50 eV is comparable to the width of about 2 eV of the Nb $4d_{z^2}$ band in 2H-NbS_2.

Bands near the Fermi level with mainly SnS character at Γ have energies of −0.40, −0.75, −1.17 eV, etc. Thus SnS-derived bands occur in the misfit-layer compound at Γ not too far below the Fermi level. On the other hand, in the band structure of SnS-1 the top of the valence band is not at the Γ point, and the energy at Γ is 1.6 eV below the top of the valence band. As a consequence one expects that the top of the valence band of the SnS part in the misfit-layer compound will be above the Fermi energy. This leads to the presence of holes in the valence bands of the SnS subsystem.

In $(SnS)_{1.20}NbS_2$ and 2H-NbS_2 the distance between the Fermi level and the bottom of the Nb $4d_{z^2}$ band is 0.70 and 0.46 eV, respectively. This indicates a larger occupation of the Nb $4d_{z^2}$ band in the misfit compound, which

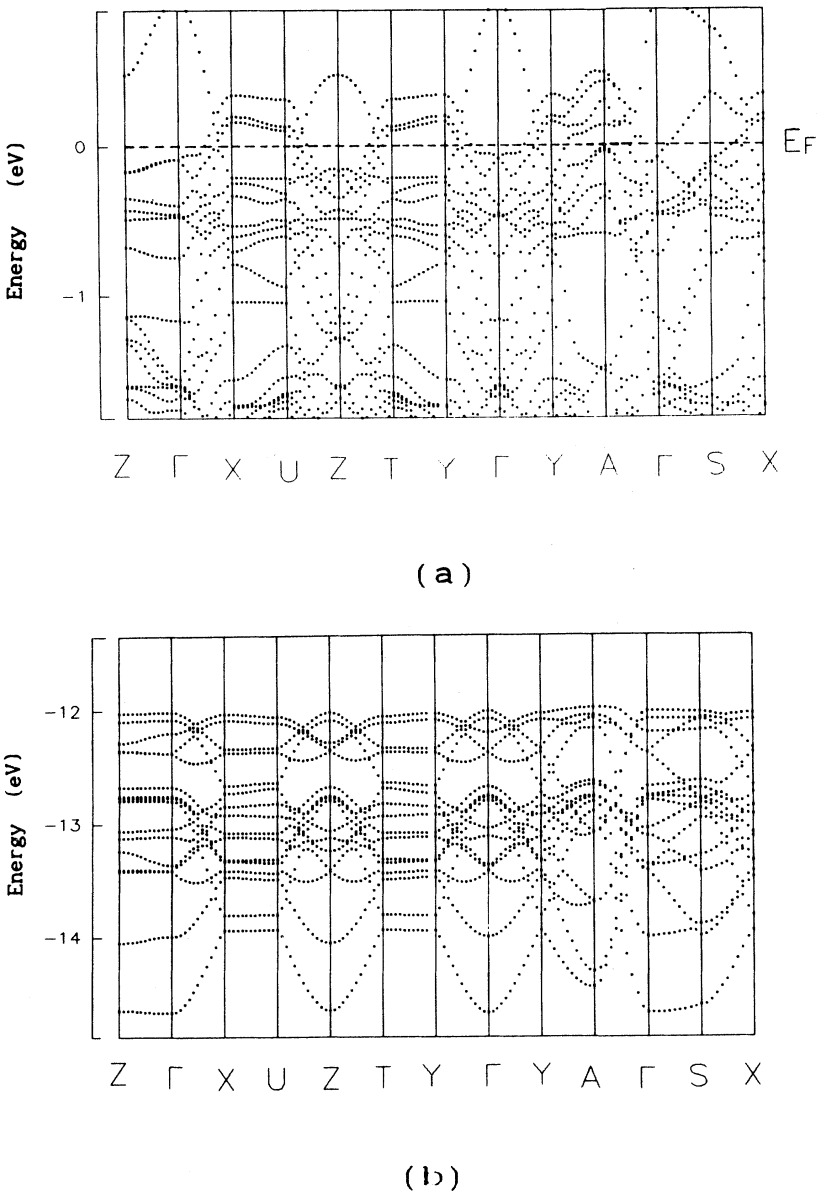

FIG. 9. Dispersion of (a) the energy bands near the Fermi level and (b) the sulfur 3*s* bands for $(SnS)_{1.20}NbS_2$.

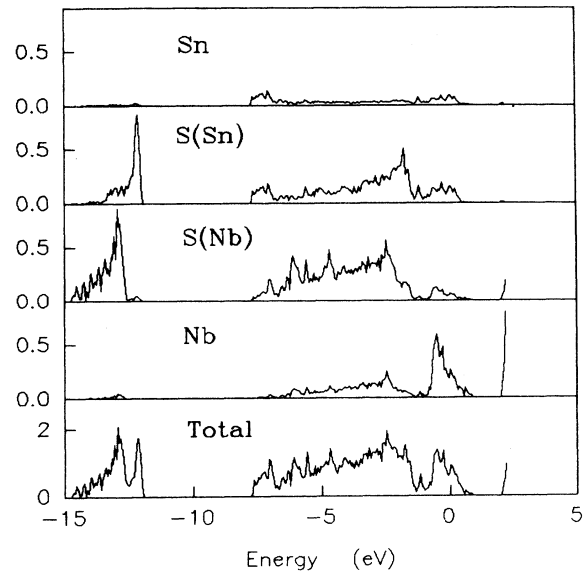

FIG. 10. Total and partial densities of states of $(SnS)_{1.20}NbS_2$; S atoms in the SnS and NbS_2 subsystems are indicated as S(Sn) and S(Nb), respectively.

must be due to the transfer of electrons from the SnS to the NbS_2 subsystem. Assuming that the DOS at the Fermi level is mainly due to the Nb $4d_{z^2}$ band, we estimate a charge transfer of 0.36 electron per Nb.

Additional evidence for charge transfer can be obtained from the position of SnS derived bands with respect to the Fermi level. In SnS-1 the top of the S $3s$ band is at -12.5 eV with respect to the top of the valence band. In the misfit-layer compound the top of the S $3s$ band of the SnS subsystem is 11.9 eV below the Fermi level. If we assume the distance between the top of S $3s$ band and the top of the valence band to be the same in the two cases, we deduce that the top of the valence band of the SnS subsystem in the misfit-layer compound is about 0.6 eV above the Fermi level. The same value is obtained if we compare the position of the bottom of the conduction band in SnS-1 (0.6 eV above the top of the valence band) with that in the misfit compound (1.0 eV above Fermi level).

We have tried to interpret the Fermi surface of the misfit-layer compound in terms of the band structures of the two components SnS and NbS_2, in order to find out whether a simple superposition of the energy bands of SnS-2 and 2H-NbS_2 can be used as a basis for describing the transport properties of the misfit-layer compound. For this purpose we used the calculated band structure to obtain the Fermi surface of 2H-NbS_2 with a hole concentration $p_1 = 1 - \Delta n = 0.6$ hole/Nb; this takes account of a charge transfer of $\Delta n = 0.4$ electron from the SnS to NbS_2 subsystem. Next we calculated the Fermi surface of SnS-2 with a hole of concentration $p_2 = \Delta n / 1.2$ (per formula unit SnS). The Fermi surfaces of SnS-2 and 2H-NbS_2, obtained in this way, were mapped onto the Brillouin zone of $(SnS)_{1.20}NbS_2$. The result was compared with the Fermi surface of $(SnS)_{1.20}NbS_2$ deduced from the calculated band structure. We found little relation between the two; apparently there is no simple relation between the Fermi surface of $(SnS)_{1.20}NbS_2$ and the Fermi surfaces of the component SnS and NbS_2. This proves that also at the Fermi surface there is considerable covalent mixing of wave functions of the two subsystems. We conclude that it is not possible to describe the transport properties of the misfit-layer compound as a simple superposition of the transport of the charge carriers in the two subsystems after charge transfer has taken place.

V. XPS AND UPS EXPERIMENTS

X-ray photoelectron spectroscopy measurements of the misfit-layer compound $(SnS)_{1.17}NbS_2$ have been reported by Ohno for the valence band[7] and by Ettema and Haas for the core levels.[8] However, the valence band was measured by Ohno with quite low resolution and the S $3s$ band was affected by the Mg $K\alpha_{3,4}$ satellites of Sn $4d$ core electrons (binding energies of 24.8 and 25.7 eV).

The misfit-layer compound $(SnS)_{1.17}NbS_2$ was synthesized and crystals were grown by vapor transport as described before.[4] Crystals obtained were approximately squares with rounded sides, with dimensions of about 2–10 mm. We carried out XPS measurements in a small spot ESCA machine of vacuum generators. A spot size of 300–600 μm was used. The radiation source was an Al anode using the $K\alpha$ line with a photon energy of 1486.6 eV. The sample surface was cleaned by stripping with Scotch tape in the preparation chamber at a base pressure of 10^{-9} Torr. The sample with a fresh surface was transported to the main chamber (base pressure 10^{-10} Torr). The cleaned surface showed hardly any contamination by oxygen and carbon. We also performed ultraviolet photoelectron spectroscopy (UPS) measurements with photons of energy 21.2 eV from a helium lamp.

The XPS core levels correspond quite well to those reported by Ettema and Haas.[8] XPS of the valence band of the misfit-layer compound $(SnS)_{1.17}NbS_2$ is shown in Fig. 11. A calculated spectrum deduced from the band structure is included for comparison. The calculated spectrum is obtained from the partial densities of states by multi-

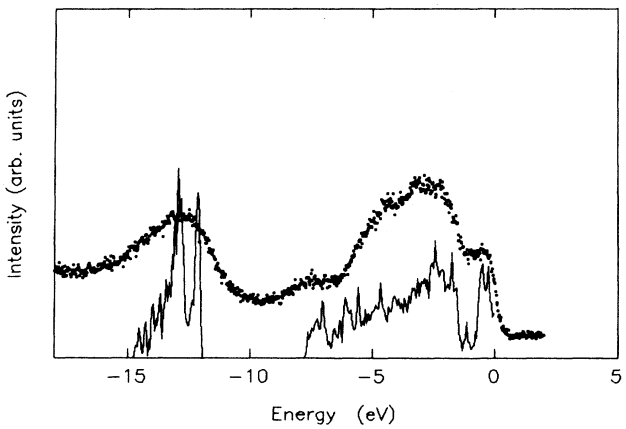

FIG. 11. XPS of the valence band of $(SnS)_{1.17}NbS_2$ (dots), compared with the calculated spectrum of $(SnS)_{1.20}NbS_2$.

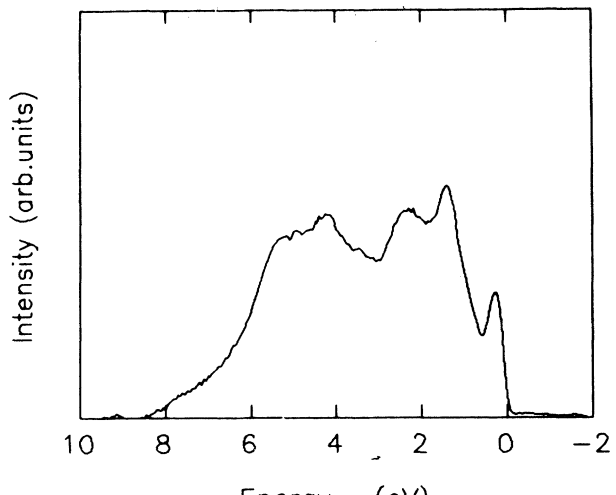

FIG. 12. UPS (photon energy 21.2 eV) of the valence band of $(SnS)_{1.17}NbS_2$ (after subtracting the background).

plying with the appropriate cross section for photoemission [for XPS with photon energy 1486.6 eV, the cross sections are 0.0012 for Sn 5*s*, 0.000 77 for Sn 5*p*, 0.0019 for S 3*s*, 0.0010 for S 3*p*, and 0.0026 for Nb 4*d* (Ref. 24)]. The valence band corresponds approximately to that reported by Ohno,[7] but there are some differences. The S 3*s* band of the spectra is quite wide, and ranges from about −16 eV to about −10.5 eV. The maximum is situated at about −12.6 eV, which agrees quite well with the peaks of the calculated spectrum [−12.9 eV of S(Nb) 3*s* and −12.1 eV of S(Sn) 3*s*]. This peak could not be seen in the spectra reported by Ohno due to the effect of the Mg $K\alpha_{3,4}$ satellites of Sn 4*d* core electrons (binding energy 24.8 and 25.7 eV). The valence band of XPS begins at −8.8 eV. There is a broad peak situated at about −7.5 eV, which corresponds to Sn 5*s* orbitals hybridized with S 3*p* (SnS part) and mixed with some S 3*p* states from the NbS_2 part. There is a narrow peak just below the Fermi level that corresponds mainly to Nb $4d_{z^2}$ states. Considering the resolution of the measurements (about 1.5 eV for this case) the calculated bands are in general agreement with the experimental data. However, the photoemission intensity in the lower part of the valence band, between energies of −8.8 and −6.5 eV, is lower than expected from the calculated spectrum. This might be due to a top layer of NbS_2 rather than SnS of the surface of the misfit-layer compound.

Figure 12 shows the UPS of the valence band of $(SnS)_{1.17}NbS_2$. The UPS corresponds quite well to the results of XPS, but the resolution is much better. The first sharp peak below the Fermi level is again the Nb $4d_{z^2}$ band. The lower valence band at about −7.5 eV has almost disappeared in the UPS spectrum, as a result of the low Sn 5*s* cross section [for UPS with photon energy 21.2 eV, the cross section is 22.10 for Nb 4*d*, 4.333 for S 3*p*, 0.065 for Sn 5*s*, and 1.173 for Sn 5*p* (Ref. 24)].

VI. DISCUSSION

The misfit-layer compounds $(MX)_{1+x}TX_2$ form a large class of intergrowth compounds with a remarkable stability. The compounds are easily prepared from the elements at high temperature (of the order of magnitude of 800 °C). The crystals show long-range order, and the number of stacking faults is limited.

An interesting question concerns the origin of the stability: What is the nature and strength of the interlayer bonding? In the transition-metal dichalcogenides the interlayer bonding is due to weak van der Waals interactions. In intercalation compounds of alkali atoms in transition-metal dichalcogenides A_xTX_2 the interlayer interaction is increased by the electrostatic interaction between positively charged A^+ ions and the negatively charged TX_2^{-x} layers. In the misfit-layer compounds there is evidence for charge transfer so that the alternating layers become charged. The stability of the misfit-layer compounds could be due to the electrostatic interaction between layers. However, it was also suggested that charge transfer is small, and that the interlayer bonding is due mainly to covalent bonds between the two subsystems.[8]

First we discuss the evidence for charge transfer in the misfit-layer compounds and the contribution of charge transfer to the interlayer bonding. Ohno[7] deduced an increased occupation of the Nb $4d_{z^2}$ band, indicating charge transfer from the SnS to the NbS_2 subsystem. In a recent paper Ettema and Haas[8] reported a study of XPS core levels of the misfit-layer compounds. From the fact that the core levels of Sn and Pb are nearly the same in $(SnS)_{1+x}TS_2$ (T = Nb, Ta, Ti) and $(PbS)_{1+x}TS_2$ (T = Nb, Ta, Ti) as in SnS and PbS, respectively, it was concluded that the Pb and Sn atoms in all these compounds are divalent and that there is no significant charge transfer. The latter conclusion was based on the assumption that the Fermi level in SnS (and PbS) in high vacuum is in the conduction band. Apparently this assumption is not justified. We found that the Fermi level in the misfit-layer compounds lies below the top of the valence band of the SnS subsystem. The equal energy of the core levels in the misfit-layer compounds and SnS then indicates that in SnS the Fermi level is in the valence band, i.e., *p*-type SnS. This is also consistent with the behavior of bulk SnS, which is always *p* type as a result of the presence of Sn vacancies.[25]

From a comparison of the calculated band structures of $(SnS)_{1.20}NbS_2$ and SnS and 2H-NbS_2 we concluded to a transfer of about $\Delta n \cong 0.4$ electron per Nb from the SnS to the NbS_2 subsystem. This charge transfer leads to charges $+0.4e$ of the SnS layers, and $-0.4e$ of the NbS_2 layers [charges per formula unit $(SnS)_{1.20}NbS_2$]. The electrostatic interlayer bonding will be of the order of $\Delta E(\text{interlayer}) \cong (e\Delta n)^2/\varepsilon d$, where d is the distance between the layers ($d = 0.5c$), and ε is an effective dielectric constant which takes into account the screening of the interactions. If we use for ε the value $\varepsilon_\infty \cong 10$,[26] we obtain $\Delta E(\text{interlayer}) \cong 0.02$ eV per formula unit; without screening ($\varepsilon = 1$) we find $\Delta E(\text{interlayer}) \cong 0.2$ eV.

The band-structure calculations show that there is co-

valent bonding between the two subsystems. In particular the distances between Sn atoms and S atoms of the NbS_2 are fairly short, leading to covalent bonds of appreciable strength (see Table III).

It is of interest to compare different cases of interlayer bonding of double layers MX (Table VIII). The simplest case is to consider cubic PbS as a stacking of double layers, held together by interlayer bonds. Because the total valence of Pb is two, and all six Pb-S bonds are equivalent in cubic PbS, the value of the bond valence corresponding to "interlayer" bonds is $\frac{1}{6}\times 2=\frac{1}{3}$. The interlayer bond in α- and β-SnS is quite weak, with a valence of 0.07–0.08. In the misfit-layer compounds with M =Sn, Pb, Bi, the interlayer bonding is much stronger, and of comparable strength with the bonding in PbS. Interlayer bonding is particularly strong in $(LaS)_{1.14}NbS_2$.

We can obtain an estimate of the interlayer binding energy ΔE(interlayer) from the cohesive energy of the pure compounds MX. Let the binding energy of an M-X bond with bond valence V_i be given by $V_i E_0$. Because for MX with M =Pb, Sn; X =S, Se, $\sum V_i=2$, the cohesive energy of the MX compound is given by $E_{\rm coh}(MX)=2E_0$. The cohesive energy, i.e., the enthalpy of formation of MX from the atoms M and X, is also given by

$$E_{\rm coh}(MX)=-\Delta H_f^0(MX)+H_0(M)+H_0(X)\ ,$$

where $\Delta H_f^0(MX)$ is the standard heat of formation of MX from the elements, and $H_0(M)$ and $H_0(X)$ represent the heats of formation of gaseous atoms M and X from the elements in the standard states. With the values H_0(Pb)=2.03 eV, H_0(Sn)=3.14 eV, H_0(S)=2.88 eV, and ΔH_f^0(PbS)=−0.98 eV, and ΔH_f^0(SnS)=−0.81 eV,[27] we obtain E_0(PbS)=$1/2E_{\rm coh}$(PbS)=2.94 eV and E_0(SnS) =$1/2E_{\rm coh}$(SnS)=3.41 eV. With these data the interlayer binding energies ΔE(interlayer) are easily calculated from the interlayer contributions V to the valence of the M atoms (Table VIII, see Ref. 28). We estimated for the electrostatic interlayer energy due to charge transfer a value between 0.02 and 0.2 eV per formula unit. We conclude that the contribution of covalent Sn-S bonds between the SnS and NbS_2 subsystems is much larger than the electrostatic interactions resulting from charge transfer.

TABLE VIII. Interlayer bond valences $V(M)$ and interlayer binding energy per M atom ΔE(interlayer)$=VE_0$ in MX and $(MX)_{1+x}TX_2$ compounds.

Compound	V	ΔE(interlayer) (in eV per Sn,Pb)
PbS (cubic)	0.333	0.98
α-SnS	0.079	0.27
β-SnS	0.072	0.25
$(SnS)_{1.20}NbS_2$	0.245	0.84
$(PbS)_{1.18}TiS_2$	0.29	0.85
$(BiSe)_{1.09}TaS_2$	0.39	
$(LaS)_{1.14}NbS_2$	0.93	

VII. CONCLUSIONS

Using a self-consistent LSW method, the electronic structure of the layer compound $(SnS)_{1.20}NbS_2$ was calculated. The results were compared with the electronic structures of the components SnS-2 and NbS_2. From these studies we find that the band structure of the misfit compound $(SnS)_{1.17}NbS_2$ can be regarded approximately as a superposition of the bands of the two components. There is a small transfer of about 0.4 electron per Nb from the SnS to the NbS_2 subsystem. The dispersion of some of the energy bands for directions $\mathbf{k}\|\mathbf{c}^*$ shows that there is a considerable covalent interaction between the two subsystems. Using the valence bond method we find that the interlayer interactions in $(SnS)_{1+x}NbS_2$ are much stronger than in α- and β-SnS. The stability of the misfit-layer compound $(SnS)_{1+x}NbS_2$ is mainly due to covalent bonding between Sn atoms and S atoms of the NbS_2 subsystem. The contribution of electrostatic interactions, as a result of charge transfer, is much smaller. The calculated electronic structure is in good agreement with experimental XPS and UPS results.

[1] G. A. Wiegers and A. Meerschaut, in *Incommensurate Sandwiched Layered Compounds,* edited by A. Meerschaut, Materials Science Forum Vols. 100 & 101 (Trans Tech, Aedermannsdorf, Switzerland, 1992).

[2] G. A. Wiegers and A. Meerschaut, J. Alloys Comp. **178**, 351 (1992).

[3] S. van Smaalen, in *Incommensurate Sandwiched Layered Compounds* (Ref. 1).

[4] G. A. Wiegers, A. Meetsma, R. J. Haange, and J. L. de Boer, Mater. Res. Bull. **23**, 1551 (1988).

[5] A. Meetsma, G. A. Wiegers, R. J. Haange, and J. L. de Boer, Acta Crystallogr. Sect. A **45**, 285 (1989).

[6] S. van Smaalen, J. Phys. Condens. Matter **1**, 2791 (1989).

[7] Y. Ohno, Phys. Rev. B **44**, 1281 (1991).

[8] A. R. H. F. Ettema and C. Haas, J. Phys. Condens. Matter **5**, 3817 (1993).

[9] M. Hangyo, T. Nishio, S. Nakashima, Y. Ohno, T. Terashima, and N. Kojima, Jpn. J. Appl. Phys. Suppl. **32-3**, 581 (1993).

[10] M. Hangyo, S. Nakashima, Y. Hamado, T. Nishio, and Y. Ohno, Phys. Rev. B **48**, 11 291 (1993).

[11] S. van Smaalen, A. Meetsma, G. A. Wiegers, and J. L. de Boer, Acta Crystallogr. Sect. B **47**, 314 (1991).

[12] I. D. Brown and D. Altermatt, Acta Crystallogr. Sect. B **41**, 244 (1985).

[13] N. E. Brese and M. O'Keeffe, Acta Crystallogr. Sect. B **47**, 192 (1991).

[14] A. R. H. F. Ettema, R. A. de Groot, C. Haas, and T. S. Turner, Phys. Rev. B **46**, 7363 (1992).

[15] H. van Leuken, A. Lodder, M. T. Czyzyk, F. Springelkamp, and R. A. de Groot, Phys. Rev. B **41**, 5613 (1990).

[16] A. R. Williams, J. Kübler, and C. D. Gelatt, Jr., Phys. Rev. B **19**, 6094 (1979).

[17] L. Hedin and B. I. Lundqvist, J. Phys. C **4**, 2064 (1971).

[18] O. K. Anderson and O. Jesepsen, Phys. Rev. Lett. **53**, 2571

(1984).
[19]C. de Lange and T. Janssen, Phys. Rev. B **28**, 195 (1983).
[20]R. V. Kasowski, Phys. Rev. Lett. **30**, 1175 (1973).
[21]W. G. Fisher and M. J. Sienko, Inorg. Chem. **19**, 39 (1980).
[22]L. F. Mattheiss, Phys. Rev. B **8**, 3719 (1973).
[23]E. Doni and R. Girlanda, in *Electronic Structure and Electronic Transitions in Layered Materials,* edited by V. Grasso (Kluwer, Dordrecht, 1984).
[24]J. J. Yeh and I. Lindau, At. Data Nucl. Data Tables **32**, 1 (1985).
[25]W. Albers, C. Haas, H. J. Vink, and J. D. Wasscher, J. Appl. Phys. Suppl. **33**, 2220 (1961).
[26]C. H. Rüscher, C. Haas, S. van Smaalen, and G. A. Wiegers, J. Phys. Condens. Matter **6**, 2117 (1994).
[27]*CRC Handbook of Chemistry and Physics,* 61st ed. (CRC, Boca Raton, FL, 1980).
[28]V. Petricek, I. Cisarova, J. L. de Boer, W. Zhou, A. Meetsma, G. A. Wiegers, and S. van Smaalen, Acta Crystallogr. Sect. B **49**, 258 (1993).